

<https://helda.helsinki.fi>

---

## Role of retinal pigment epithelium permeability in drug transfer between posterior eye segment and systemic blood circulation

Ramsay, Eva

2019-10

---

Ramsay , E , Hagström , M , Vellonen , K-S , Boman , S , Toropainen , E , del Amo , E M , Kidron , H , Urtti , A & Ruponen , M 2019 , ' Role of retinal pigment epithelium permeability in drug transfer between posterior eye segment and systemic blood circulation ' , European Journal of Pharmaceutics and Biopharmaceutics , vol. 143 , pp. 18-23 . <https://doi.org/10.1016/j.ejpb.2019.08.008>

---

<http://hdl.handle.net/10138/318291>

<https://doi.org/10.1016/j.ejpb.2019.08.008>

---

cc\_by\_nc\_nd

acceptedVersion

---

*Downloaded from Helda, University of Helsinki institutional repository.*

*This is an electronic reprint of the original article.*

*This reprint may differ from the original in pagination and typographic detail.*

*Please cite the original version.*

# Role of retinal pigment epithelium permeability in drug transfer between posterior eye segment and systemic blood circulation

Eva Ramsay <sup>a,b</sup>, Marja Hagström <sup>b</sup>, Kati-Sisko Vellonen<sup>a</sup>, Susanna Boman <sup>c</sup>, Elisa Toropainen <sup>a</sup>, Eva M. del Amo <sup>d</sup>, Heidi Kidron <sup>b</sup>, Arto Urtti <sup>a,b,e</sup> and Marika Ruponen <sup>a</sup>

<sup>a</sup> School of Pharmacy, Faculty of Health Sciences, University of Eastern Finland, FI-70211 Kuopio, Finland.

<sup>b</sup> Drug Research Program, Division of Pharmaceutical Biosciences, Faculty of Pharmacy, University of Helsinki, P.O. Box 56, FI-00014 Helsinki, Finland.

<sup>c</sup> Finnish Food Authority, Ruokavirasto, Kuvornöörinkatu 27, 83500 Outokumpu, Finland

<sup>d</sup> School of Pharmacy, University of Manchester, Manchester, United Kingdom.

<sup>e</sup> Laboratory of Biohybrid Technologies, Institute of Chemistry, St Petersburg State University, 198504 Petergof, Russia.

**Key words:** retinal pigment epithelium; intravitreal clearance; ex vivo; permeability; bovine; blood-retina barrier; ocular pharmacokinetics

## Abstract

Retinal pigment epithelium (RPE) is a major part of blood-retinal barrier that affects drug elimination from the vitreous to the blood and drug distribution from blood circulation into the eye. Even though drug clearance from the vitreous has been well studied, the role of RPE in the process has not been quantified. The aim of this work was to study the role of RPE clearance ( $CL_{RPE}$ ) as part of drug elimination from the vitreous and ocular drug distribution from the systemic blood circulation. We determined the bidirectional permeability of eight small molecular weight drugs and bevacizumab antibody across isolated bovine RPE-choroid. Permeability of small molecules was  $10^{-6} - 10^{-5}$  cm/s showing 13-15 fold range of outward and inward permeation, while permeability of bevacizumab was lower by 2-3 orders of magnitude. Most small molecular weight drugs showed comparable outward (vitreous-to-choroid) and inward (choroid-to-vitreous) permeability across the RPE-choroid, except ciprofloxacin and ketorolac that had an over 6 and 14-fold higher outward than inward permeability, respectively, possibly indicating active transport. Six of seven tested small molecular weight drugs had outward  $CL_{RPE}$  values that were comparable with their intravitreal clearance ( $CL_{IVT}$ ) values (0.84-2.6 fold difference). On the contrary, bevacizumab had an outward  $CL_{RPE}$  that was only 3.5% of the  $CL_{IVT}$ , proving that its main route of elimination (after intravitreal injection) is not RPE permeation. Experimental values were used in pharmacokinetic simulations to assess the role of the RPE in drug transfer from the systemic blood circulation to the vitreous ( $CL_{BV}$ ). We conclude that for small molecular weight drugs the RPE is an important route in drug transfer between the vitreal cavity and blood, whereas it effectively hinders the movement of bevacizumab from the vitreous to the systemic circulation.

## 44 1. Introduction

45

46 The prevalence of age-related diseases at the back of the eye, such as age-related macular degeneration (AMD),  
47 diabetic retinopathy, glaucoma and macular edema is constantly growing. The diseases with neovascular  
48 changes, such as exudative AMD are treated with anti-VEGF compounds, such as Fab-fragment ranibizumab  
49 (Lucentis®), soluble receptor aflibercept (Eylea®), and antibody bevacizumab (off-label use of Avastin®). Other  
50 potential drugs for the treatment of neovascularization include tyrosine kinase inhibitors, aptamers, and siRNA <sup>1</sup>.  
51 Inflammations associated with diabetic macular edema, AMD, and uveitis, are treated with corticosteroids, such  
52 as triamcinolone acetonide and dexamethasone <sup>2</sup>. Drug treatment of these diseases is accomplished with  
53 intravitreal administration of drug solutions, suspensions or implants. Even though intravitreal injections are  
54 invasive they are the method-of-choice in the retinal drug treatment, because topical, subconjunctival and systemic  
55 drug administrations do not provide adequate drug delivery to the retina <sup>3</sup>.

56

57 After an intravitreal injection, the drug diffuses in the vitreous humour and distributes to the neighboring tissues.  
58 All drugs are capable of diffusing from the vitreous to the anterior chamber and then eliminate from the eye via  
59 aqueous humor outflow <sup>4</sup>. Additionally, the drugs may be eliminated from the vitreous posteriorly, across the blood-  
60 ocular barriers, if the compound has adequate membrane permeability based on its molecular properties (e.g.  
61 size, lipophilicity) <sup>5</sup>. Blood-ocular barriers include two main components: blood-aqueous barrier (BAB) and blood-  
62 retinal barrier (BRB). The BRB consists of retinal pigment epithelium (RPE) and the endothelium of the retinal  
63 vessels, whereas the BAB is formed by the posterior iris epithelium, iridial capillaries, ciliary muscle capillaries,  
64 and nonpigmented ciliary epithelium. Inter-cellular tight-junctions are found both in the BAB and the BRB, limiting  
65 the size of the paracellular space to about 2 nm (diameter) and restricting the molecular transfer between the eye  
66 and blood circulation <sup>3,6</sup>.

67

68 The RPE is situated between the retinal photoreceptors and choroid, and it is essential for the function of the  
69 retina, maintaining the homeostasis between the neural retina and blood circulation of the fenestrated choroidal  
70 blood vessels. Due to its large surface area, the RPE is considered to be an important route of elimination of small  
71 molecular weight drugs <sup>3</sup>. After crossing the neural retina and RPE, the choroid acts as an eliminating sink,  
72 because the leaky choroidal vessels have high blood flow. Small molecules may cross the RPE transcellularly and  
73 paracellularly, and they have wide range of intravitreal clearance values (0.031 – 1.530 ml/h) <sup>5</sup> that depend on the  
74 ability of the compounds to permeate across the blood ocular barriers. Due to their poor permeation of the BRB,  
75 intravitreally injected proteins and other macromolecules are mainly eliminated from the vitreous to the aqueous  
76 humor outflow, resulting in low intravitreal clearance values of 0.011 – 0.071 ml/h <sup>5</sup>. In principle, drugs may cross  
77 the RPE by passive permeation and/or active transport, depending on drug concentration, expression and  
78 localization of transporters, and affinity of drug to the transporter protein. So far, evidence suggests that passive  
79 permeability is the main mechanism of drug clearance across the BRB. Recently, the RPE transporters were  
80 quantitated <sup>7,8</sup>, but the clinical role of RPE transporters is still unclear <sup>9</sup>.

81

82 The knowledge of the intravitreal pharmacokinetics is important in order to develop efficient retinal drug treatments  
83 as intravitreal injections or implants <sup>5</sup>. Furthermore, drug permeability in the BRB is a key parameter in defining  
84 distribution of drugs from the blood circulation to the posterior eye segment <sup>10</sup>. A reliable quantitative structure-  
85 property relationship model (QSPR) was developed for clearance of small molecular weight drugs between  
86 vitreous and blood circulation <sup>5</sup>. However, intravitreal clearance values do not provide information about the routes  
87 of vitreal drug elimination. Previously, permeability of some  $\beta$ -blocking agents and FITC-dextran were  
88 investigated in isolated bovine RPE-choroid <sup>11</sup>, which demonstrated the effects of the molecular size and  
89 lipophilicity ( $\log D_{7.4}$ ) on permeability. In this study, we extended this approach to eight small molecular weight  
90 drugs and one protein drug, bevacizumab (Avastin®). To our understanding RPE permeability for such drug set  
91 (with broad lipophilicity and molecular weight range) has not been previously reported in the literature. The  
92 experimental permeability values and *in vivo* intravitreal clearance values from rabbits were used to estimate the  
93 role of the RPE as intravitreal route of drug elimination and distribution route from the systemic blood circulation.

94

## 95 **2. Materials and Methods**

96

### 97 *2.1 Drug molecules*

98

99 Eight small molecular weight drugs and one protein drug were chosen for the permeability study (Table 1). The  
100 cassette mixture of the small molecular weight drugs was prepared by combining the individual stock solutions  
101 (Table 1) and diluting with a balanced salt solution BSS Plus (Alcon Laboratories, TX, USA) containing 7.14 mg/ml  
102 sodium chloride, 0.38 mg/ml potassium chloride, 0.154 mg/ml calcium chloride dihydrate, 0.2 mg/ml  
103 magnesium chloride hexahydrate, 0.42 mg/ml, dibasic sodium phosphate, 2.1 mg/ml sodium bicarbonate,  
104 0.92 mg/ml dextrose, 0.184 mg/ml glutathione disulfide, and supplemented with 10 mM Hepes (pH 7.4). The  
105 drug concentration in the cassette mixture stock solution was either 20 or 200  $\mu\text{g/ml}$ , depending on the analytical  
106 limit of quantification. The concentrations of aztreonam, ganciclovir, and quinidine were 200  $\mu\text{g/ml}$ , whereas the  
107 other compounds were used at concentration of 20  $\mu\text{g/ml}$ .

108

109

110

111

112

113

114

115

116

117

118

119

120 Table 1. Drug molecules in the permeability study.

Drug molecules	Stock solution	Manufacturer
Aztreonam	10 mg/ml in DMSO	Fluka, China
Ciprofloxacin	0.5 mg/ml in 0.1 M HCl	BioChemica, China
Fluconazole	10 mg/ml in DMSO	Sigma-Aldrich, St.Louis, MO, USA
Ganciclovir	10 mg/ml in DMSO	Sigma-Aldrich, St.Louis, MO, USA
Ketorolac Tris salt	1 mg/ml in PBS	Sigma-Aldrich, St.Louis, MO, USA
Methotrexate	1 mg/ml in DMSO	Fluka, USA
Quinidine	10 mg/ml in DMSO	Sigma-Aldrich, Steinheim, Germany
Voriconazole	10 mg/ml in DMSO	Fluka, Steinheim, Germany
Bevacizumab	Avastin® 25 mg/ml	Roche Pharma AG, Grenzach-Wyhlen, Germany

121

122

123 *2.2 Tissue preparation*

124

125 Freshly enucleated bovine eyes (> 1 year old animals) were obtained from a local slaughterhouse and delivered  
 126 to the lab in CO<sub>2</sub> Independent Medium (Gibco, Life Technologies). The eyes were first cleaned of muscle and fat  
 127 tissue surrounding the eye. Then the anterior part of the eye was removed by cutting circumferentially  
 128 approximately 8 mm posterior from the limbus. The vitreous was gently removed from the remaining eye cup that  
 129 was cut in three parts. Medium was added on the tissues to avoid drying. The neural retina was gently removed  
 130 using forceps and, thereafter, the RPE-choroid was carefully isolated from sclera using scissors and curved  
 131 forceps, avoiding the area of the optic nerve.

132

133 *2.3 Permeability study*

134

135 The isolated RPE-choroid was placed on a plastic mesh (1 mm pore size) and further located between two ring  
 136 shaped silicon adapters with a circular aperture of 0.64 cm<sup>2</sup>. The silicon adapters with the tissue was placed in a  
 137 vertical Ussing/diffusion chamber (NaviCyte, Harvard Apparatus, Holliston, MA). The chamber parts in contact with  
 138 the silicon adapters had been treated with vacuum grease to avoid edge leakage during the experiment. BSS Plus  
 139 supplemented with 10 mM Hepes (pH 7.4) buffer was added to both sides of the chambers; 5 ml in the cassette  
 140 mixture experiments and 4 ml in the bevacizumab experiments. Both sides of the chambers were attached to gas  
 141 tubing, supplying the tissue with gas (5% CO<sub>2</sub>, 10% O<sub>2</sub>, and 85% N<sub>2</sub>) at a rate of 3-4 bubbles/s. The bubbling  
 142 mixed the buffer solution and maintained the pH at 7.4. The chambers were maintained at 37 °C with a heating  
 143 block and circulating water bath (Grant Instruments Ltd, Cambridge, England). The chambers were equipped with  
 144 electrode caps and glass barrel Ag/AgCl electrodes (NaviCyte Electrodes; Harvard Apparatus) that were  
 145 connected to a voltage-current clamp (VCC MC6; Physiologic Instruments, San Diego, CA) for transepithelial  
 146 electrical resistance (TER) measurements as described previously <sup>12</sup>.

147

148 Permeability of the cassette mixture drugs was studied in outward and inward directions. The outward direction  
149 mimics vitreous-to-choroid permeation (apical to basolateral), whereas the inward permeation models choroid-to-  
150 vitreous distribution (basolateral to apical side). The bevacizumab permeability was studied only in the outward  
151 direction. The permeability experiments were initiated by replacing 500-700  $\mu$ l of drug solution to the donor side  
152 (cassette mix or bevacizumab). The drug concentrations in the donor side were 20 or 200  $\mu$ g/ml in the cassette  
153 mix. Bevacizumab concentration in the donor side was 4.4 mg/ml. In the cassette mix study, samples of 500  $\mu$ l  
154 were withdrawn from the receiver site at 15, 30, 45, 60, 75, 90, 120, 150, 180, 210, 240, 270, 300, 330, and 360  
155 min and replaced with blanc buffer. Additionally, samples of 40  $\mu$ l were withdrawn from the donor side in the  
156 beginning and at the end of the experiment. The samples were stored in -20  $^{\circ}$ C for later LC-MS/MS analysis. In  
157 the bevacizumab study, samples of 100  $\mu$ l were withdrawn from the receiver site at 180, 240, 270, 300, 330, 360,  
158 390, and 420 min and replaced with blanc buffer. Samples of 10  $\mu$ l were withdrawn from the donor side in the  
159 beginning and at the end of the experiment. These samples were stored overnight in + 4  $^{\circ}$ C and analyzed next  
160 day by ELISA.

161  
162 The apparent permeability coefficients ( $P_{app}$ ) of the eight small molecular weight drugs and bevacizumab were  
163 calculated (Eq. 1) as:

$$164 \quad P_{app, RPE-choroid} \text{ (cm/s)} = J / C_0 \quad \text{Eq.1}$$

165  
166 Where J (ng/cm<sup>2</sup>\*s) is the drug flux across the exposed membrane area (A=0.64 cm<sup>2</sup>) in the linear range and C<sub>0</sub>  
167 is the initial drug concentration in the donor compartment (ng/cm<sup>3</sup>). The sink conditions were maintained during  
168 the permeability experiments (i.e. drug concentration in the receiver side was below 10% of the donor side  
169 concentration).

## 170 171 2.4 Quantitative analyses

### 172 173 2.4.1 Small molecular drugs

174  
175 The concentrations of the small molecular weight drugs in the cassette mix were analyzed with a slightly modified  
176 UPLC-MS/MS technique from previous study <sup>12</sup>. Minimum of eight standard curve points and blank control were  
177 used for quantitation of the compounds. Standard curve included all eight analytes and the following four  
178 deuterated internal standards: atenolol-d7, ganciclovir-d5, methotrexate-d3, and lincomycin-d3. The method was  
179 validated by including four quality control samples in three parallel sets. The linearity range varied from 1 to 1000  
180 ng/ml depending of the compound, and limit of quantitation (LOQ) was set to the lowest concentration in the  
181 standard curve for each drug. The linear concentration range for each drug is presented in Supplementary material  
182 (Table 1).

183  
184 Liquid chromatography separations were carried out using Waters Acquity UPLC instrument, with the flow through  
185 needle injection system (Waters, MA, USA) coupled with Agilent Poroshell 120 SB-C18 (2.1 x 50 mm, 2.7  $\mu$ m)

186 column (Agilent Technologies, Inc., DE, USA) at 50 °C. The mobile phase consisted of 0.1% of formic acid in  
187 ultrapure water (A) and 100% of LC-MS grade acetonitrile (B). The gradient elution started with 2% of B at 0-1 min  
188 and continued with 2-95% of B at 1-5 min. Total run time was 9.5 min including flush and equilibration of the  
189 column. The flow-rate was set to 0.3 ml/min and injection volume to 0.3 µl. After every sample two wash injections,  
190 composed of a mixture of ultrapure water and isopropanol including 0.1 % formic acid, were performed to prevent  
191 any carry over.

192 Mass spectrometry measurements were carried out using a Waters Xevo triple quadrupole mass spectrometer  
193 (TQ-S) equipped with an ESI source (Waters) operated in positive ionization mode. The optimal source parameters  
194 were: capillary voltage 3.5 V, cone voltage 2 V, source temperature 150 °C, desolvation temperature 500 °C.  
195 Nitrogen (Aga, Helsinki, Finland) was used as desolvation gas (800 L h<sup>-1</sup>) and cone gas (150 L h<sup>-1</sup>), argon (Aga,  
196 Helsinki, Finland) was used as collision gas (0.15 ml/min). The multiple reaction monitoring (MRM) mode was  
197 used for quantification. The precursor and fragment ions of the small molecular weight drugs and the internal  
198 standards (with their collision energies) are presented in Supplementary material (Table 2). The resulting data was  
199 analyzed with Waters MassLynx software V4.1

200

#### 201 2.4.2 *Bevacizumab*

202

203 The concentration of bevacizumab was analyzed with a BioSim™ Bevacizumab (Avastin®) (Human) ELISA Kit  
204 (E4373-100, BioVision, CA, USA) using manufacturer's protocol. The standards were prepared in BSS Plus (10  
205 mM Hepes) buffer. The reliability of the method was checked by preparing standards also to the manufacturer's  
206 Assay Buffer.

207

208 Stability of bevacizumab was analyzed in different conditions for 6 hours to assure protein stability in the  
209 permeability studies (Table 2). Stability of bevacizumab was analyze with ELISA assays.

210

211 Table 2. Conditions of bevacizumab stability studies.

Concentration	Buffer	Temperature	Gas*	Comments
5.7 mg/ml	BSS Plus (10 mM Hepes)	37 °C	yes	Permeability assay conditions
3 mg/ml	BSS Plus (10 mM Hepes)	37 °C	no	
3 mg/ml	BSS Plus (10 mM Hepes)	25 °C	no	
3 mg/ml	0.9% NaCl	25 °C	no	48 h stability guaranteed by the manufacturer

212 \*5% CO<sub>2</sub>, 10% O<sub>2</sub>, and 85% N<sub>2</sub> gas

213

214

215

216

217 2.5 Calculation of RPE clearance

218

219 Contribution of RPE as elimination route from the vitreous or as a distribution route from the systemic blood  
 220 circulation was estimated by calculating clearance via RPE ( $CL_{RPE}$ ; ml/h) (Eq. 2 and Eq. 3):

221

222 outward  $CL_{RPE} = \text{outward } P_{app, RPE-choroid} \times S_{RPE}$  vitreous-to-choroid Eq.2

223 inward  $CL_{RPE} = \text{inward } P_{app, RPE-choroid} \times S_{RPE}$  choroid-to-vitreous Eq.3

224

225 where  $P_{app, RPE}$  is the drug permeability (cm/s) in the RPE-choroid and  $S_{RPE}$  is the surface area of the rabbit RPE  
 226 ( $5.2 \text{ cm}^2$ )<sup>13</sup>.

227

228 2.6. Simulations on ocular drug entry through the RPE

229

230 The simulations were performed using the modified model from Vellonen et al., (2016)<sup>10</sup> (Fig. 1). In the model drug  
 231 transfer between systemic blood circulation and vitreal cavity was assumed to be dictated by the distribution  
 232 clearance between the blood circulation and eye ( $CL_{BV}$ ). The clearance for drug elimination from the vitreous  
 233 ( $CL_{IVT}$ ) for ciprofloxacin, fluconazole and methotrexate were obtained from *in vivo* rabbit studies as calculated in  
 234 del Amo et al (2015). The  $CL_{BV}$  was obtained 1) by assuming drug entry only via the RPE using inward  $CL_{RPE}$   
 235 (Equation 3) or 2) by assuming all routes of entry ( $CL_{IVT}$ ) into the vitreous. The drug may enter the vitreous from  
 236 the systemic blood circulation across the BRB and BAB. Intravitreal drug concentrations were simulated for  
 237 ciprofloxacin, methotrexate, and fluconazole using RPE entry or total entry scenarios. Only free drug was assumed  
 238 to permeate across the blood ocular barriers. The fractions of free drug and protein bound drug in the plasma and  
 239 vitreous were obtained from the literature<sup>10,14</sup>. A more detailed structure of the model, including equations and  
 240 model parameters can be found from Supplementary material (Fig. 1 and Table 3).

241

242

243

244

245

246

247

248

249

250

251

252

253

254

255

256

257

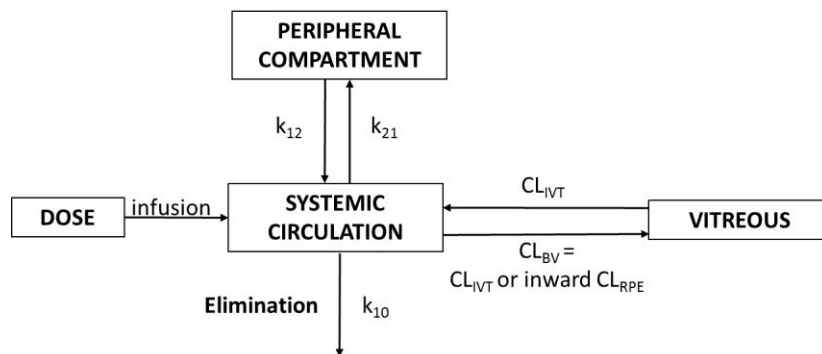


Figure 1. The compartmental model used for simulating intravitreal drug concentration after systemic drug administration, adapted to the calculated inward RPE clearance values.



258 **3. Results**

259

260 **3.1 Drug permeability**

261

262 Overall drug permeabilities in the *ex vivo* RPE-choroid experiments ranged over 3 orders of magnitude (from  
263 ketorolac and voriconazole to bevacizumab) indicating that the membrane was tight and intact (Table 3). The  
264 integrity of the RPE-choroid was also confirmed at the beginning of the experiments by transepithelial resistance  
265 (TER) measurements, which was  $102 \pm 55 \Omega \times \text{cm}^2$  (n=22).

266

267 Among small molecules the range of permeability values was 13-15 fold for outward and inward permeation, also  
268 suggesting proper barrier properties (Table 3). Hydrophilic aztreonam ( $\text{LogD}_{7.4}$ : - 4.32) had 5-times lower  
269 permeability ( $4\text{--}5 \times 10^{-6} \text{ cm/s}$ ) than lipophilic voriconazole ( $\text{LogD}_{7.4}$ : 1.21;  $20\text{--}25 \times 10^{-6} \text{ cm/s}$ ). The results of  
270 quinidine are not reported, because the mass balance was incomplete. Outward and inward permeability values  
271 in the isolated bovine RPE-choroid were in the same range for 5 compounds (Table 3, Fig. 2). Ciprofloxacin and  
272 ketorolac showed preferred directionality for outward permeation (Table 3; Fig. 1).

273

274 Bevacizumab (molecular weight 149 kDa) had 100- to 200-fold lower permeability than hydrophilic small molecules  
275 (aztreonam, methotrexate) and 2000 times slower outward permeation than ketorolac. The stability experiments  
276 showed that bevacizumab was stable in the permeability studies (results in Supplementary material, Table 4).

277

278 Table 3. Permeability data from the experiments with isolated RPE-choroid tissues.

Drug	LogD <sub>7.4</sub> *	Molecular weight	Outward P <sub>app, RPE-choroid</sub> x 10 <sup>-6</sup> cm/s	Inward P <sub>app, RPE-choroid</sub> x 10 <sup>-6</sup> cm/s	Outward/Inward P <sub>app, RPE-choroid</sub> ratio**
Aztreonam	- 4.32	435.4	5.37 ± 5.19 (n= 8)	4.47 ± 2.62 (n= 9)	1.2
Ciprofloxacin	- 0.29	331.3	9.52 ± 5.28 (n= 7)	1.43 ± 0.77 (n= 8)	6.7
Fluconazole	0.45	306.3	15.64 ± 4.66 (n= 8)	12.95 ± 2.69 (n= 9)	1.2
Ganciclovir	- 1.61	255.2	9.70 ± 7.90 (n= 8)	6.49 ± 3.97 (n= 9)	1.5
Ketorolac	- 0.34	255.3	69.21 ± 31.9 (n= 8)	4.78 ± 3.99 (n= 9)	14.5
Methotrexate	- 5.1	454.4	9.39 ± 2.74 (n= 8)	4.54 ± 2.99 (n= 8)	2.1
Voriconazole	1.21	349.3	25.00 ± 6.12 (n= 8)	21.02 ± 4.21 (n= 9)	1.2
Bevacizumab		149 000	0.035 ± 0.020 (n= 4)		

279 \*LogD<sub>7.4</sub> values are computational (ACDLabs® software, version 12; Advanced Chemistry Development, Inc.,  
280 Toronto, Canada)

281 \*\* The outward/inward ratio is calculated based on the mean values of outward and inward P<sub>app, RPE-choroid</sub>

282

283

284

285

286

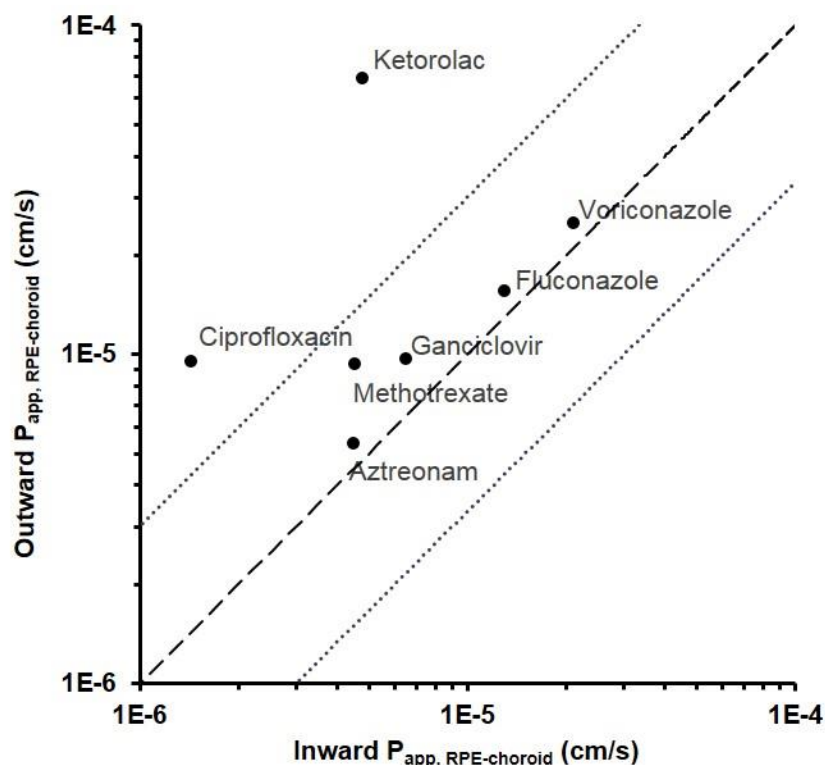


Figure 2. The outward versus inward RPE-choroid permeability of the cassette dose drugs (n= 7-9). The dashed line represents identical permeabilities without directionality. The dotted lines show the situations in which inward  $P_{app, RPE-choroid}$  is either 3-fold lower or 3-fold higher than outward  $P_{app, RPE-choroid}$ .

### 3.2 Estimated drug clearance across the RPE

The outward permeability (vitreous-to-choroid) values were used to calculate drug clearance across the RPE-choroid (outward  $CL_{RPE}$ ) (Table 4). These values were compared to *in vivo* intravitreal clearance ( $CL_{IVT}$ ) values in the rabbit eye<sup>5</sup> (Table 4; Fig. 3). For most drugs outward  $CL_{RPE}$  values were within 2.6 fold range from  $CL_{IVT}$  values (Fig. 3, Table 4). The high outward permeability of ketorolac resulted in an outward  $CL_{RPE}$  value that was five times higher than the  $CL_{IVT}$ . Low outward permeability of bevacizumab resulted in low  $CL_{RPE}$  (about 0.035 x  $CL_{IVT}$ ).

Table 4. The intravitreal clearance ( $CL_{IVT}$ ) in rabbit<sup>5</sup> and the calculated (Eq. 2) outward RPE-choroid clearance ( $CL_{RPE}$ ) of the cassette dose drugs and bevacizumab.

Drug	$CL_{IVT}$ (ml/h) in rabbit <sup>5</sup>	outward $CL_{RPE}$ (ml/h)	$CL_{IVT}/CL_{RPE}$	$(CL_{RPE}/CL_{IVT}) \times 100\%$
Aztreonam	0.125	0.101 ± 0.097	1.2	81
Ciprofloxacin	0.336	0.178 ± 0.099	1.9	53
Fluconazole	0.753	0.293 ± 0.087	2.6	39
Ganciclovir	0.153	0.182 ± 0.148	0.84	119
Ketorolac	0.283	1.296 ± 0.597	0.22	458
Methotrexate	0.197	0.176 ± 0.051	1.1	89
Voriconazole	0.421	0.468 ± 0.115	0.90	111
Bevacizumab	0.019	0.000657 ± 0.000365	29	3.5

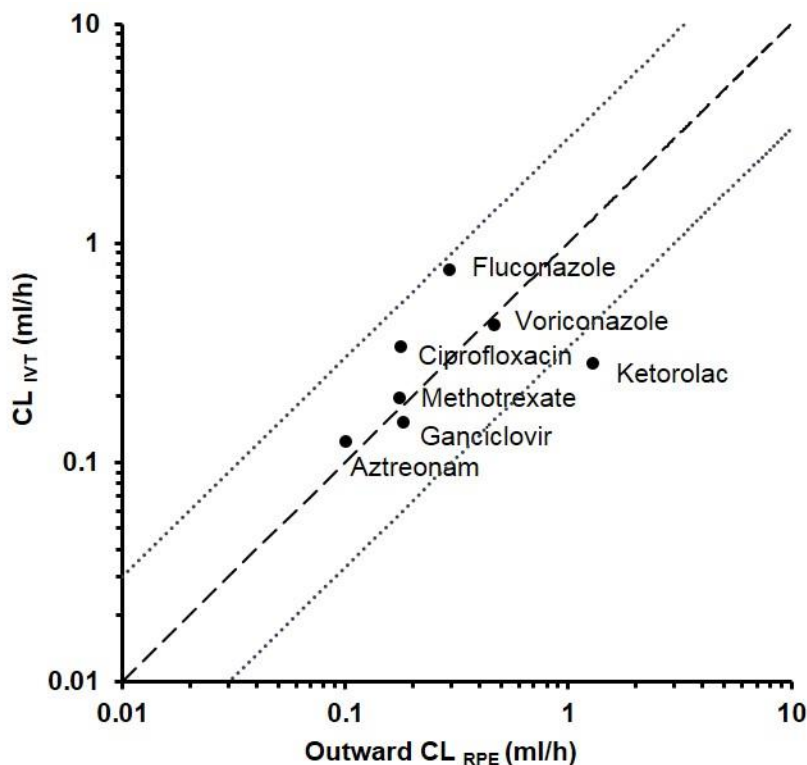


Figure 3. Experimental intravitreal drug clearance in rabbits *in vivo* ( $CL_{IVT}$ ) versus calculated outward RPE clearance ( $CL_{RPE}$ ) from this study. The dashed line represents identical values for  $CL_{RPE}$  and  $CL_{IVT}$ . The dotted lines show the situations in which outward  $CL_{RPE}$  is either 3-fold lower or 3-fold higher than  $CL_{IVT}$ .

### 3.3. Simulations on the RPE contribution in ocular entry of systemic drugs

Contribution of the RPE as the ocular entry route from systemic blood circulation was simulated by comparing two situations:  $CL_{BV}$  equals the inward  $CL_{RPE}$  (entry only via RPE) or  $CL_{IVT}$  (entry via all possible routes, across the BRB and BAB). In both cases, drug elimination from the vitreous was simulated using the *in vivo* intravitreal clearance ( $CL_{IVT}$ ) values (including all routes of elimination) instead of the calculated outward clearance values across the RPE (outward  $CL_{RPE}$ ). Table 5 shows the simulated approximate AUC values for ciprofloxacin, methotrexate, and fluconazole. The contribution of RPE as the route of entry varies among the compounds: ciprofloxacin 8%, methotrexate 43% and fluconazole 32%. Since these three compounds show higher outward than inward permeability in the RPE, it seems that in many cases the RPE has more important contribution on intravitreal drug elimination than on the drug distribution from the blood stream into the vitreous.

377 Table 5. Simulated AUC values in the vitreous after systemic delivery of ciprofloxacin 100 mg, methotrexate 12.5  
 378 mg and fluconazole 50 mg, assuming drug distribution from the blood circulation to the vitreous (CL<sub>BV</sub>) equal to  
 379 inward CL<sub>RPE</sub> (1) or equal to CL<sub>LIVT</sub> (2).

Ocular entry route	CL <sub>BV</sub>	AUC (µg x h/ml) in vitreous		
		Ciprofloxacin	Methotrexate	Fluconazole
1. Only RPE	Inward CL <sub>RPE</sub> *	1.56	15.89	19.85
2. All routes	CL <sub>LIVT</sub>	19.60	36.85	61.65

380 \* Inward CL<sub>RPE</sub> values for ciprofloxacin (0.0268 ml/h), methotrexate (0.0850 ml/h) and, fluconazole (0.242ml/h)  
 381 were based on the experimental values. Inward CL<sub>RPE</sub> values were based on equation 3: inward CL<sub>RPE</sub> = inward  
 382  $P_{app, RPE-choroid} \times S_{RPE}$   
 383

384

#### 385 4. Discussion

386

387 Intravitreal injection is the most commonly used route of drug administration for the treatment of the posterior eye  
 388 segment<sup>3</sup>. The typical range of intravitreal clearance values for small and large molecular weight compounds have  
 389 been earlier defined and their routes of elimination have been proposed<sup>5</sup>. However, only permeability studies can  
 390 give a clear insight of the route of elimination of these compounds from the vitreous. Likewise, drug entry from the  
 391 blood circulation into the vitreous has been characterized and modeled<sup>10</sup>, but the role of RPE in ocular drug entry  
 392 has not been explored.

393

394 Based on the results, most of the small molecular weight drugs showed a similar outward CL<sub>RPE</sub> and CL<sub>LIVT</sub>, which  
 395 illustrates that the RPE is their main elimination route from the vitreous after intravitreal injection. Mostly the CL<sub>LIVT</sub>  
 396 values were slightly higher than the calculated outward CL<sub>RPE</sub> values. This is most probably due to the presence  
 397 of other elimination routes *in vivo*, such as aqueous humour outflow, ciliary body, and iris. On the contrary, the  
 398 outward CL<sub>RPE</sub> for bevacizumab (149 kDa) was only 3.5% of its intravitreal clearance, which is in line with the  
 399 conclusions drawn by del Amo et al., (2017), stating that only 3-20% of macromolecules (MW 4-80 kDa) are  
 400 eliminated across the RPE. Hutton-Smith et al., (2017) reached similar conclusions with a three-compartment  
 401 semi-mechanistic model for estimating retinal permeability (RPE and inner limiting membrane) of IgG, IgG null, Fc  
 402 and Fab fragment. They concluded that 13-18% of these are eliminated across the RPE and the rest via other  
 403 routes.

404

405 Rabbit is the most commonly used animal model in ocular *in vivo* pharmacokinetic studies and therefore intravitreal  
 406 clearance data is mainly available from this specie. However, bovine eyes were chosen as the animal model for  
 407 permeability studies due to easy isolation of the RPE-choroid from bovine eyes. The RPE was isolated together  
 408 or partly with the underlying choroid, but choroid is a leaky layer (TER ≈ 9 Ω x cm<sup>2</sup>) that does not restrict the  
 409 permeation of solutes<sup>15</sup>. Most of the small molecular weight drugs (255 – 454 Da), excluding ciprofloxacin and  
 410 ketorolac, showed similar permeability in outward and inward directions ( $P_{app, RPE-choroid} = 10^{-6} - 10^{-5}$  cm/s), which  
 411 is an indication of passive permeability. Bevacizumab (149 kDa) had low outward permeability of 2-3 orders of  
 412 magnitude lower (10<sup>-8</sup> cm/s) than the small molecular weight drugs. To our knowledge this is the first time  
 413 experimental values of RPE permeability is been presented for the therapeutic drug, bevacizumab (Avastin®).

414 Quinidine was included in the original drug mixture, but the mass balance of quinidine was incomplete, suggesting  
415 accumulation to the cell components, such as melanosomes. The choroid and RPE are enriched in melanin, and  
416 associated with prolonged retention of quinidine in the melanosomes <sup>16,17</sup>.

417

418 Outward  $P_{app, RPE-choroid}$  of ciprofloxacin and ketorolac were 6 and 14 times higher than their inward permeability in  
419 the bovine RPE-choroid, respectively. The directional permeability could be explained by the presence of active  
420 transporters. RPE is known to express both influx and efflux transporters on both sides of the membrane <sup>7,9</sup>.  
421 Ciprofloxacin had particularly low permeability in the inward direction, compared to the other small molecular  
422 weight drugs. This might be due to binding of ciprofloxacin to efflux transporter(s) in the RPE <sup>3,18</sup>. For example,  
423 MRP4 is known to transport ciprofloxacin and it is present in the human RPE <sup>7,19</sup>. Ketorolac had much higher  
424 outward permeability than the other small molecular weight drugs, while its inward permeability was in the same  
425 range with the other drugs. This may be due to influx transporter activity on the vitreal side of the RPE. For instance  
426 OAT2 is present in human RPE <sup>7</sup> and it is capable of transporting ketorolac <sup>20</sup>. Additionally, when using a mixture  
427 of drug molecules there is a possibility for transporter related interactions. Another competing drug may interfere  
428 with the permeability of a transporter dependent drug molecule. In any case, only sparse information is available  
429 of the expression and activity of transporters in the bovine RPE <sup>9,21</sup>. Available data suggest that the transporters  
430 may only have a modest role in the pharmacokinetics of the RPE <sup>9</sup>.

431

432 The role of RPE in drug distribution from the systemic blood circulation into the vitreous was simulated with a  
433 modified model of Vellonen et al., (2016)<sup>10</sup>. The simulations showed that the RPE permeation contributes to the  
434 vitreal drug concentrations as a route of entry, but it is not necessarily a dominating one (Table 5). This could be  
435 explained by the presence of efflux transporters at the choroidal side of the RPE that may reduce the inward  
436 permeability of the drug. On the other hand, other routes of drug entry from blood circulation, such as at the BAB  
437 the nonpigmented ciliary epithelium and fenestrated vessels in the ciliary processes, could play significant role in  
438 the inward drug permeation. The nonpigmented ciliary epithelium has similar surface area as the RPE (1.4 x  
439 difference in humans <sup>3</sup>). Thus, BAB may play an important role in the distribution of small molecular weight drugs,  
440 but its pharmacokinetic role is poorly known.

441

442 The information on RPE permeability is useful in developing new ocular drugs and drug delivery systems.  
443 Information on barrier permeability will be useful in building physiologically based pharmacokinetic models and  
444 finite element models that will facilitate ocular drug development <sup>22-25</sup>.

445

## 446 **Conclusions**

447

448 Bidirectional permeability studies with excised RPE-choroid specimens were carried out with small molecular  
449 weight drugs and bevacizumab. The permeability values spanned over a range of three orders of magnitude.  
450 Permeability values were further used to calculate clearance values for drug transfer across the RPE from and  
451 into the eye. It seems that the RPE is the main elimination route for small molecular weight drugs from the vitreous,

452 and efficiently blocks permeation of macromolecules, such as bevacizumab. For systemic drugs, the RPE  
453 contribute in drug distribution to the eye, but it is not the only route.

454

#### 455 **Acknowledgements**

456

457 We gratefully acknowledge grant funding from Academy of Finland (311122) (AU). We would like to thank Maija  
458 Lahtela-Kakkonen for helping with the logistics of the bovine eyes. Lea Pirskanen is acknowledged for her skilful  
459 technical assistance. This study was supported by Leo, Mary, and Mary-Ann Hackman Foundation (ER); The  
460 Finnish Cultural Foundation (ER); Orion Research Foundation (ER); European Union's Horizon 2020 research  
461 and innovation programme under the Marie Skłodowska-Curie (grant No 799880) (EDA).

462

#### 463 **Conflict of interest**

464

465 There are no conflict of interest

466

#### 467 **References**

468

- 469 1. Zhang K, Zhang L, Weinreb RN. Ophthalmic drug discovery: novel targets and mechanisms for retinal  
470 diseases and glaucoma. *Nat Rev Drug Discov.* 2012;11(7):541-559.
- 471 2. Novack GD, Robin AL. Ocular pharmacology. *J Clin Pharmacol.* 2016;56(5):517-527.
- 472 3. del Amo EM, Rimpelä A-K, Heikkinen E, et al. Pharmacokinetic aspects of retinal drug delivery. *Prog*  
473 *Retin Eye Res.* 2017;57.
- 474 4. Maurice DM, Mishima S. Ocular Pharmacokinetics. In: Sears ML, ed. *Handbook of Experimental*  
475 *Pharmacology/ Pharmacology of the Eye.* Berlin-Heidelberg: Springer-Verlag; 1984:19-116.
- 476 5. del Amo EM, Vellonen KS, Kidron H, Urtti A. Intravitreal clearance and volume of distribution of  
477 compounds in rabbits: in silico prediction and pharmacokinetic simulations for drug development. *Eur J*  
478 *Pharm Biopharm.* 2015;95:215-226.
- 479 6. Smith RS, Rudt LA. Ocular vascular and epithelial barriers to microperoxidase. *Invest Ophthalmol Vis*  
480 *Sci.* 1975;14(7):556-560.
- 481 7. Pelkonen L, Sato K, Reinisalo M, et al. LC-MS/MS Based Quantitation of ABC and SLC Transporter  
482 Proteins in Plasma Membranes of Cultured Primary Human Retinal Pigment Epithelium Cells and  
483 Immortalized ARPE19 Cell Line. *Mol Pharm.* 2017;14(3):605-613.
- 484 8. Dahlin A, Geier E, Stocker SL, et al. Gene expression profiling of transporters in the solute carrier and  
485 ATP-binding cassette superfamilies in human eye substructures. *Mol Pharm.* 2013;10(2):650-663.
- 486 9. Vellonen KS, Hellinen L, Mannermaa E, Ruponen M, Urtti A, Kidron H. Expression, activity and  
487 pharmacokinetic impact of ocular transporters. *Adv Drug Deliv Rev.* 2018;126:3-22.
- 488 10. Vellonen KS, Soini EM, Del Amo EM, Urtti A. Prediction of ocular drug distribution from systemic blood  
489 circulation. *Mol Pharm.* 2016;13(9):2906-2911.

- 490 11. Pitkänen L, Ranta VP, Moilanen H, Urtti A. Permeability of retinal pigment epithelium: Effects of permeant  
491 molecular weight and lipophilicity. *Investig Ophthalmol Vis Sci.* 2005;46(2):641-646.
- 492 12. Ramsay E, Ruponen M, Picardat T, et al. Impact of Chemical Structure on Conjunctival Drug  
493 Permeability: Adopting Porcine Conjunctiva and Cassette Dosing for Construction of In Silico Model. *J*  
494 *Pharm Sci.* 2017;106(9):2463-2471.
- 495 13. Reichenbach A, Ziegert M, Schnitzer J, et al. Development of the rabbit retina. V. The question of  
496 "columnar units". *Brain Res Dev Brain Res.* 1994;79(1):72-84.
- 497 14. Rimpelä AK, Reunanen S, Hagström M, Kidron H, Urtti A. Binding of small molecule drugs to porcine  
498 vitreous humor. *Mol Pharm.* 2018;15(6):2174-2179.
- 499 15. Miller SS, Edelman JL. Active ion transport pathways in the bovine retinal pigment epithelium. *J Physiol.*  
500 1990;424:283-300.
- 501 16. Pelkonen L, Tengvall-Unadike U, Ruponen M, et al. Melanin binding study of clinical drugs with cassette  
502 dosing and rapid equilibrium dialysis inserts. *Eur J Pharm Sci.* 2017;109(May):162-168.
- 503 17. Rimpelä AK, Reinisalo M, Hellinen L, et al. Implications of melanin binding in ocular drug delivery. *Adv*  
504 *Drug Deliv Rev.* 2018;126:23-43.
- 505 18. DrugBank. Ciprofloxacin, transporters. <https://www.drugbank.ca/drugs/DB00537>. Published 2019.
- 506 19. Haslam IS, Wright JA, O'Reilly DA, Sherlock DJ, Coleman T, Simmons NL. Intestinal ciprofloxacin efflux:  
507 The role of breast cancer resistance protein (ABCG2). *Drug Metab Dispos.* 2011;39(12):2321-2328.
- 508 20. Mathialagan S, Piotrowski MA, Tess DA, Feng B, Litchfield J, Varma M V. Quantitative prediction of  
509 human renal clearance and drug-drug interactions of organic anion transporter substrates using in vitro  
510 transport data: A relative activity factor approach. *Drug Metab Dispos.* 2017;45(4):409-417.
- 511 21. Mannermaa E, Vellonen KS, Ryhänen T, et al. Efflux protein expression in human retinal pigment  
512 epithelium cell lines. *Pharm Res.* 2009;26(7):1785-1791.
- 513 22. Zhang Y, Bazzazi H, Lima E Silva R, et al. Three-Dimensional Transport Model for Intravitreal and  
514 Suprachoroidal Drug Injection. *Invest Ophthalmol Vis Sci.* 2018;59(12):5266-5276.
- 515 23. Hutton-Smith LA, Gaffney EA, Byrne HM, Caruso A, Maini PK, Mazer NA. Theoretical Insights into the  
516 Retinal Dynamics of Vascular Endothelial Growth Factor in Patients Treated with Ranibizumab, Based on  
517 an Ocular Pharmacokinetic/Pharmacodynamic Model. *Mol Pharm.* 2018;15(7):2770-2784.
- 518 24. Hutton-Smith LA, Gaffney EA, Byrne HM, Maini PK, Gadkar K, Mazer NA. Ocular Pharmacokinetics of  
519 Therapeutic Antibodies Given by Intravitreal Injection: Estimation of Retinal Permeabilities Using a 3-  
520 Compartment Semi-Mechanistic Model. *Mol Pharm.* 2017;14(8):2690-2696.
- 521 25. Lamminsalo M, Taskinen E, Karvinen T, et al. Extended pharmacokinetic model of the rabbit eye for  
522 intravitreal and intracameral injections of macromolecules: quantitative analysis of anterior and posterior  
523 elimination pathways. *Pharm Res.* 2018;35(153).
- 524